



POLITEHNICA UNIVERSITY OF BUCHAREST

Doctoral School of Aerospace Engineering

PHD THESIS SUMMARY

Optimal Control of Multi-Agent Systems with Flight Formations Applications

Eng. Serena Cristiana VOICU (STOICU)

2023

Contents

1	Introduction.....	3
2	Linear Quadratic Design.....	4
2.1	Preliminaries – LQR Problem Formulation; Graph Theory.....	4
2.2	Centralised Control	4
2.3	Distributed Control.....	5
3	Case Studies – Linear Quadratic Design	6
3.1	Centralised Control	6
3.2	Distributed Control.....	7
4	H_∞ Design.....	10
4.1	Preliminaries - H_∞ Design	10
4.2	Centralised Control	10
4.3	Distributed Control.....	11
5	Case Studies - H_∞ Design.....	12
5.1	H_∞ Design in case of ideal communication channels	12
5.1.1.	Centralised Control	12
5.1.2.	Distributed Control	13
5.2	H_∞ Design in case of time delays communication network	15
5.2.1.	Centralised Control	15
5.2.2.	Distributed Control	15
5.3	H_∞ Design in case of failure communication	16
5.3.1.	Situation I.....	17
5.3.2.	Situation II	18
6	H_∞ Design for stochastic systems with Markov Chains.....	19
6.1	Case of single agent.....	20
6.2	Multi-agent systems	20
7	Case Studies - H_∞ Design with Markov Chains	21
7.1	$N = 100$ agents.....	22
7.2	$N = 3$ agents	23
8	Results and Concluding Remarks	24
9	References.....	25

Key words: multi-agent systems, centralised control, distributed control, stochastic systems with Markov chains, H_∞ design, time-delays

1 Introduction

The progress of new technologies in the last decades had as a result the significant development of multi-agent systems (MAS). This concept refers to the coordinated flight of two or more vehicles, called agents, for which various characteristics are imposed, having a common objective. Recently, the applications of these systems have achieved considerable interest, becoming a subject that has received special attention. The applicability area is continuously expanding, including both military and civil applications.

In research literature, the solutions proposed in the control of networked systems generally refer to two types of control: centralised and distributed. A comparative study of these approaches is represented by the paper [1] which includes theoretical notions related to their specific characteristics. The centralised system design involves the interconnection of all agents, which implies difficulties in data processing. This type of control requires high performance of the central controller and a single error of it influences the behaviour of the entire network. Compared to the centralised case, the distributed control assumes a specific structure, namely, the information transmission is achieved between certain pairs of agents. Significant theoretical results regarding this type of control are given in [2] and the progress on this topic is presented in [3]. Compared to the centralised case that presents difficulties in data processing, the efficiency of distributed control is observed, especially for systems with large number of agents.

Optimal control is a feature of modern control system design methods. The main aspects relate to obtaining the stability of the resultant system and satisfying certain restrictions associated with conventional control, giving the system the best characteristics for a specific model [4].

In this thesis, the attention is directed to the study of the multi-agent system control problem. Unlike a single-agent system, specific problems arise regarding the design of control systems. A characteristic of these systems refers to the information transmission realized by communication channels, introducing new challenges in terms of the automatic control system design. Considering the external factors that can affect the objectives achievement, an optimal vehicle coordination solution is needed to achieve the desired performance of the entire network. These situations involve the failure of one or more members, the time delays effects or the overloading of communication channels that ensure the information transmission causing data packet drop out. These scenarios are the objectives of this work, their effects being analysed through the presented case studies.

The paper is structured in different parts as follows. Chapter 1 is a preliminary chapter presenting general considerations regarding previous approaches to the multi-agent system control problem and the main objectives of this thesis. The first method used in this study, linear quadratic regulator (LQR), is analysed in Chapter 2, establishing the specific aspects of the two types of control (centralised and distributed). The optimal control addressed in Chapter 3 aims to determine the solutions of the linear quadratic problem in the two considered cases, for which the decoupled dynamics of a vehicle is used. Chapter 4 formulates a detailed description of H_∞ design for the two types of control. Chapter 5 is dedicated to the comprehensive exposition of case studies both in the situation of ideal communication between agents and in various scenarios that consider the

imperfections of information transmission channels. Chapter 6 gives the results of the H_∞ design where the data packet drop out in the communication networks is represented by the Markov process. The relevant design steps for stochastic systems are formulated for systems consisting of N agents with identical dynamics. The last part of the case studies, described in Chapter 7, illustrates the capabilities of the H_∞ controller for stochastic systems taking into account possible network data packet losses, using Markov processes. The characteristics of this design type are highlighted by the obtained time evolutions of two different flight configurations. Chapter 8 relieves, through the stated conclusions, the results offered by the design methods proposed in this thesis.

2 Linear Quadratic Design

2.1 Preliminaries – LQR Problem Formulation; Graph Theory

- **LQR Problem Formulation**

Considering the linear system of an aerial vehicle of form:

$$\dot{x}(t) = Ax(t) + Bu(t) \text{ with } x(0) = x_0 \quad (2.1)$$

where x is the state vector, u is the control vector, and the cost function defined as:

$$J(u) = \int_0^\infty (x^T(t)Qx(t) + u^T(t)Ru(t))dt \quad (2.2)$$

with the weighting matrices $Q \geq 0$ and $R > 0$, it is reminded that solving the linear quadratic problem consists in determining the optimal controller of form $u(t) = -Kx(t)$ that minimises the cost function (2.2).

- **Graph Theory**

The flight of an agent network involves the coordination of several aerial vehicles for which their interconnection is defined by graph theory, the communication mode being explained in matrix form. Any graph is defined by specific matrix forms used in the stability analysis of flight formation members, detailed in [5].

2.2 Centralised Control

This chapter focuses on centralised control problem that involves communication between each pair of agents in both directions. To describe the necessary model to solve the linear quadratic problem, the dynamics of the system composed of N interconnected subsystems is defined. The cost function of the linear quadratic problem for N agents includes the dynamic behaviour of the systems, being defined as follows:

$$J(u, x_0) = \int_0^\infty \left(\sum_{i=1}^N (x_i(t)^T Q_{ii} x_i(t) + u_i(t)^T R_{ii} u_i(t)) + \sum_{i=1}^N \sum_{j \neq i}^N (x_i(t) - x_j(t))^T Q_{ij} (x_i(t) - x_j(t)) \right) dt. \quad (2.3)$$

This can be rewritten as:

$$J(u(t), x_0) = \int_0^\infty (x^T(t)Q_f x(t) + u^T(t)R_f u(t))dt \quad (2.4)$$

Taking into account the initial conditions, the control law that minimizes the cost function (2.4) is defined as:

$$u = -R_f^{-1}B_f^T P_f x \quad (2.5)$$

where P_f represents the positive definite symmetric stabilising solution of the equation:

$$A_f^T P_f + P_f A_f - P_f B_f R_f^{-1} B_f^T P_f + Q_f = 0. \quad (2.6)$$

2.3 Distributed Control

Considering the main disadvantage of centralised control that needs to access information from all agents, the design of a distributed control is needed. Compared to the centralised case, distributed control requires a certain structure, namely, the communication is realized between certain agents, this fact being possible due to the controllers interconnection.

The paper [6] proposes a method to determine a suboptimal distributed controller for which it is necessary to define the interconnection way of the agents. Thus, a positive definite symmetric matrix denoted $M \in \mathbb{R}^{N \times N}$ is introduced. The work demonstrates different ways of defining this matrix so that the system stability can be achieved. It is necessary to establish the minimum size for which the linear quadratic problem can be solved, given by the term $N_\ell = d_{max} + 1$, where d_{max} represents the maximum number of connections for a node. Reference [6] sets various conditions for choosing the matrix M .

It is necessary to determine the positive definite symmetric solution P_ℓ of the ARE associated with the centralised LQR problem of reduced size, corresponding to a number of $N_\ell = d_{max}(\mathcal{G}) + 1$ agents.

$$A_\ell^T P_\ell + P_\ell A_\ell - P_\ell B_\ell R_\ell^{-1} B_\ell^T P_\ell + Q_\ell = 0 \quad (2.7)$$

where P_ℓ is of form:

$$P_\ell = \begin{bmatrix} P_{\ell_{11}} & P_{\ell_{12}} & \cdots & P_{\ell_{12}} \\ P_{\ell_{12}} & P_{\ell_{11}} & \cdots & P_{\ell_{12}} \\ \vdots & \vdots & \ddots & \vdots \\ P_{\ell_{12}} & P_{\ell_{12}} & \cdots & P_{\ell_{11}} \end{bmatrix}. \quad (2.8)$$

To determine the positive definite symmetric solution P needed to obtain the controller, the Riccati algebraic equation associated with the linear quadratic problem for a single agent is solved:

$$A^T P + P A - P B R^{-1} B^T P + Q_1 = 0. \quad (2.9)$$

Furthermore, $P_{\ell_{11}} = P - (N_\ell - 1)P_{\ell_{12}}$. The corresponding optimal controller has the following structure:

$$K_\ell = \begin{bmatrix} K_1 & K_2 & \cdots & K_2 \\ K_2 & K_1 & \cdots & K_2 \\ \vdots & \vdots & \ddots & \vdots \\ K_2 & K_2 & \cdots & K_1 \end{bmatrix}. \quad (2.10)$$

3 Case Studies – Linear Quadratic Design

In the presented case studies, the two types of controller are analysed: centralised and distributed. In order to study the agents' evolutions for the considered networks, the numerical simulations use the decoupled dynamics of an aerial unmanned vehicle (UAV), thus the performances of members for both longitudinal and lateral dynamics are analysed. In the considered case studies, the linearized state space equations of a vehicle are used.

The longitudinal motion of an aerial vehicle is characterized by the decoupled equations for the following states, $x = [u \ w \ q \ \theta \ h]^T$, whose state space expression is given by:

$$[\dot{u} \ \dot{w} \ \dot{q} \ \dot{\theta} \ \dot{h}]^T = A_{long}[u \ w \ q \ \theta \ h]^T + B_{long} \begin{bmatrix} \delta_E \\ \delta_T \end{bmatrix}. \quad (3.1)$$

The matrix values corresponding to the longitudinal dynamics of an unmanned aerial vehicle are considered, according to [7]. In the lateral dynamics case, the state space system is defined by the five corresponding states $x = [v \ p \ r \ \varphi \ \psi]^T$ as follows:

$$[\dot{v} \ \dot{p} \ \dot{r} \ \dot{\varphi} \ \dot{\psi}]^T = A_{lat}[v \ p \ r \ \varphi \ \psi]^T + B_{lat} \begin{bmatrix} \delta_A \\ \delta_R \end{bmatrix}. \quad (3.2)$$

3.1 Centralised Control

- **Longitudinal Dynamics**

The four identical aerial vehicles of the network are assumed to have null initial conditions. The entire network is required to reach a desired altitude $h = 10 \text{ m}$ and velocity $u = 3 \text{ m/s}$. Figure 3.1 and Figure 3.2 illustrate the time responses of the controlled system using linear quadratic method considering null initial conditions for each agent.

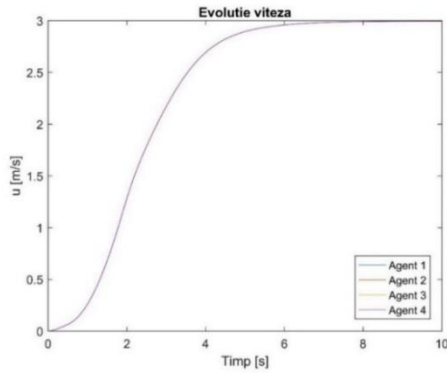


Figure 3.1 Time evolution of velocity – centralised control

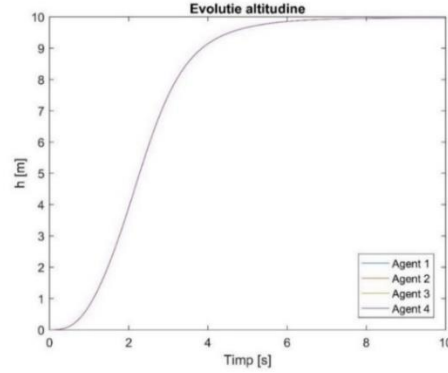


Figure 3.2 Time evolution of altitude – centralised control

- **Lateral dynamics**

For the presented numerical simulations, the four aerial vehicles of the configuration are considered to have different initial conditions: the velocities v and yaw angles ψ . To obtain the simulations in Figure 3.3, different initial velocities are imposed and the desired result is to reach and maintain a certain velocity value. This figure illustrates the time evolution of velocity where it can be observed that the networked agents reach the desired value, taking into consideration the different initial values. For the developments in Figure 3.4, the initial yaw angle value for each agent is assumed to be null. It can be seen that the entire network stabilises at the desired value in a few seconds, maintaining it throughout the simulation.

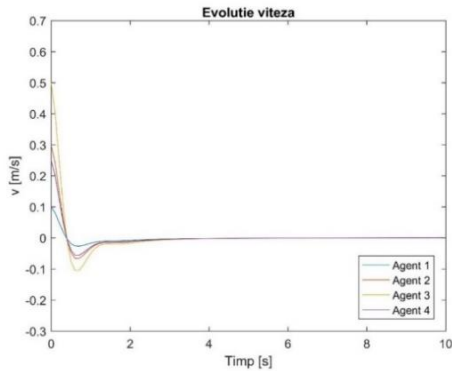


Figure 3.3 Time evolution of velocity – centralised control

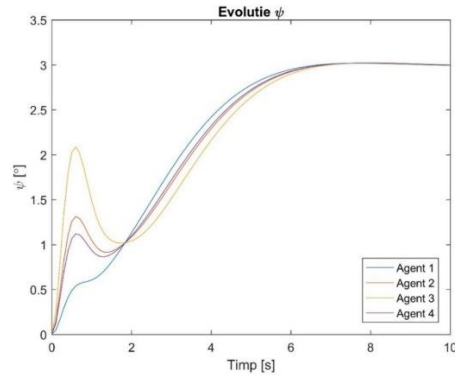


Figure 3.4 Time evolution of ψ – centralised control

3.2 Distributed Control

To study the characteristics of distributed control and to relieve the controller capabilities, two different configurations, illustrated in Figure 3.5 and Figure 3.6, are studied.

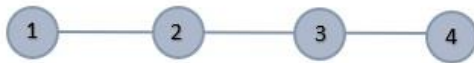


Figure 3.5 Configuration A

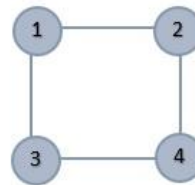


Figure 3.6 Configuration B

3.2.1. Longitudinal Dynamics

- **Configuration A**

In order to analyse the longitudinal dynamics in the distributed control case, an aerial vehicles formation consisting of 4 agents with the configuration in Figure 3.5 is considered. The information transmission between agents is defined by the corresponding adjacency matrix with the expression (3.3).

$$\mathcal{A}(\mathcal{G}) = \begin{bmatrix} 0 & 1 & 0 & 0 \\ 1 & 0 & 1 & 0 \\ 0 & 1 & 0 & 1 \\ 0 & 0 & 1 & 0 \end{bmatrix} \quad (3.3)$$

Following the gain matrix determination, the form of the distributed controller is analysed, in which $K_{D_{13}} = K_{D_{14}} = 0, K_{D_{31}} = K_{D_{24}} = 0$ and $K_{D_{41}} = K_{D_{42}} = 0$. From Figure 3.5, it is observed that the communication between the pairs of agents (1,3) and (1,4) is not possible, which proves the existence of null terms on the corresponding position in the obtained controller. This property is proved for every agent of the network. Figure 3.7 and Figure 3.8 demonstrate the achievement of the desired performances by all networked members.

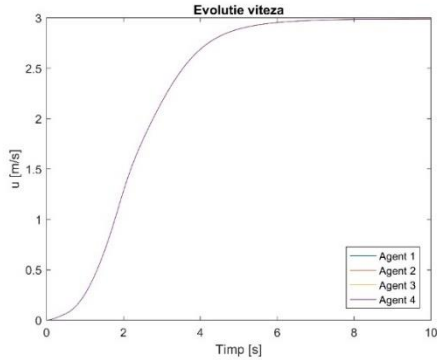


Figure 3.7 Time evolution of velocity – distributed control – Config. A

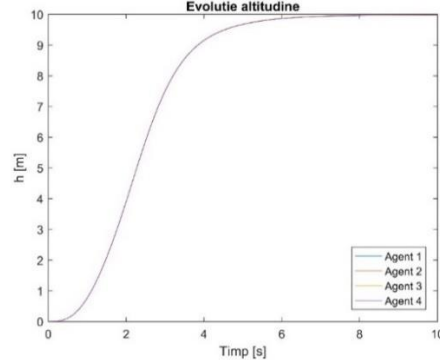


Figure 3.8 Time evolution of altitude – distributed control – Config. A

- **Configuration B**

This part of the work uses a new configuration consisting of an equal number of agents, but their arrangement and communication way are different comparative to the previous case. The analysed structure is illustrated in Figure 3.6, and the expression (3.4) defines the interconnection mode of the vehicles.

$$\mathcal{A}(\mathcal{G}) = \begin{bmatrix} 0 & 1 & 1 & 0 \\ 1 & 0 & 0 & 1 \\ 1 & 0 & 0 & 1 \\ 0 & 1 & 1 & 0 \end{bmatrix} \quad (3.4)$$

From the velocity time evolution (Figure 3.9) it can be seen that all vehicles maintain the desired velocity value $u = 3m/s$ throughout the time simulation. Figure 3.10 illustrated the behaviour of the flight formation for which it is necessary to reach the altitude value $h = 10 m$.

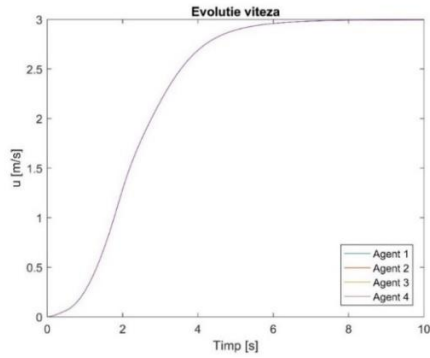


Figure 3.9 Time evolution of velocity – distributed control – Config. B

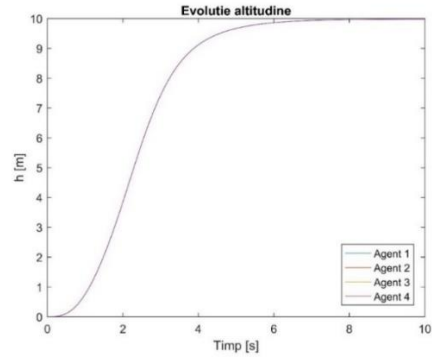


Figure 3.10 Time evolution of altitude – distributed control – Config. B

3.2.2. Lateral Dynamics

- **Configuration A**

Considering the decoupled aerial vehicle dynamics, it is required to study the lateral motion stability. The objectives involve reaching a desired velocity of the agents and maintain this value during the flight, illustrated in Figure 3.11. The numerical simulations in Figure 3.12 highlight the time response of the system in case of maintaining an imposed yaw angle value.

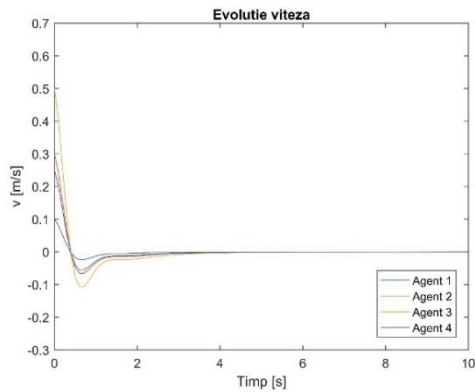


Figure 3.11 Time evolution of velocity – distributed control – Config. A

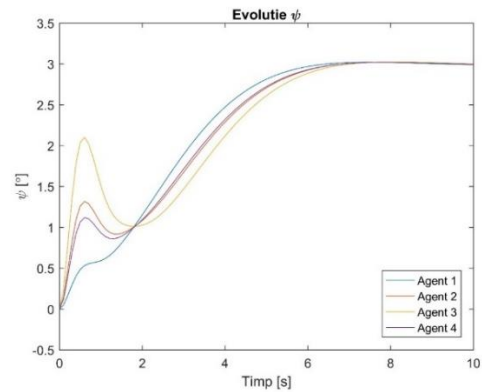


Figure 3.12 Time evolution of ψ – distributed control – Config. A

- **Configuration B**

Acquiring numerical simulations implies reaching pre-set performances. Rather, it is required that the aerial vehicles maintain desired velocity and yaw angle values throughout the simulation. Figure 3.13 and Figure 3.14 demonstrate both the system stability and the pre-set objectives achievement, taking into consideration the different initial imposed conditions.

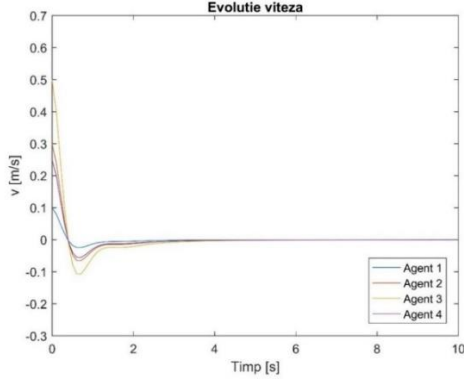


Figure 3.13 Time evolution of velocity – distributed control – Config. B

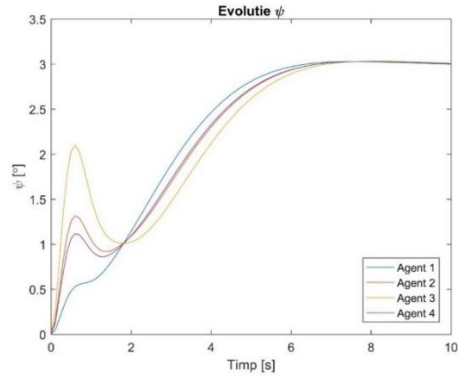


Figure 3.14 Time evolution of ψ – distributed control – Config. B

4 H_∞ Design

As a modern design technique, H_∞ theory involves determining a controller that stabilises the closed loop system and achieving a design objective by minimizing the H_∞ norm of a specific transfer function. The theoretical notions along with the specific properties are detailed treated in references [8], [9], [10].

4.1 Preliminaries - H_∞ Design

Considering a network of identical vehicles, the dynamics is written as follows:

$$\begin{aligned} \dot{x}(t) &= Ax(t) + B_1 u_1(t) + B_2 u_2(t) \\ y_1(t) &= Cx(t) + Du_2(t) \\ y_2(t) &= x(t), t \geq 0 \end{aligned} \quad (4.1)$$

where $x \in \mathbb{R}^n$ is the state vector, $u_1 \in \mathbb{R}^{m_1}$ represents the exogenous input, $u_2 \in \mathbb{R}^{m_2}$ denotes the control input, $y_1 \in \mathbb{R}^{p_1}$ stands for the quality output and y_2 is the measured output. Furthermore, to determine the solutions of H_∞ problem, two conditions are assumed to be true: $C^T D = 0$ and $D^T D = I$.

4.2 Centralised Control

The dynamic system of the formation is written in a compact form as follows:

$$\begin{aligned} \dot{\tilde{x}}(t) &= \tilde{A}\tilde{x}(t) + \tilde{B}_1 \tilde{u}_1(t) + \tilde{B}_2 \tilde{u}_2(t) \\ \tilde{y}_1(t) &= \tilde{C}\tilde{x}(t) + \tilde{D}\tilde{u}_2(t) \\ \tilde{y}_2(t) &= \tilde{x}(t), t \geq 0 \end{aligned} \quad (4.2)$$

For a given $\gamma > 0$, the following cost function is defined:

$$J(u_{1_1}, \dots, u_{1_N}, u_{2_1}, \dots, u_{2_N}) = \int_0^\infty \left[\sum_{i=1}^N (|y_{1i}(t)|^2 - \gamma^2 |u_{1i}(t)|^2) + \frac{1}{2} \sum_{i=1}^N \sum_{j=1, j \neq i}^N (x_i(t) - x_j(t))^T Q_{ij} (x_i(t) - x_j(t)) \right] dt \quad (4.3)$$

The state-feedback gain determination $\tilde{F} \in \mathbb{R}^{m_2 N \times n N}$ involves solving the Riccati equation:

$$\tilde{A}^T \tilde{X} + \tilde{X} \tilde{A} + \gamma^{-2} \tilde{X} \tilde{B}_1 \tilde{B}_1^T \tilde{X} - \tilde{X} \tilde{B}_2 \tilde{B}_2^T \tilde{X} + \tilde{Q}^T \tilde{Q} = 0 \quad (4.4)$$

where $\tilde{X} \geq 0$ is the stabilising solution. Furthermore, the stabilising solution of Riccati equation (4.4) has the following structure:

$$\tilde{X} = \begin{bmatrix} \tilde{X}_1 & \tilde{X}_2 & \cdots & \tilde{X}_2 \\ \tilde{X}_2 & \tilde{X}_1 & \cdots & \tilde{X}_2 \\ \vdots & \vdots & \ddots & \vdots \\ \tilde{X}_2 & \tilde{X}_2 & \cdots & \tilde{X}_1 \end{bmatrix} \quad (4.5)$$

where $\tilde{X}_1 = X_1 + (N-1)X_2$ and $\tilde{X}_2 = X_2$, where X_1 and X_2 are the positive semidefinite stabilising solutions to the following Riccati equations

$$A^T X_1 + X_1 A + X_1 (\gamma^{-2} B_1 B_1^T - B_2 B_2^T) X_1 + C^T C = 0 \quad (4.6)$$

$$(A + (\gamma^{-2} B_1 B_1^T - B_2 B_2^T) X_1)^T X_2 + X_2 (A + (\gamma^{-2} B_1 B_1^T - B_2 B_2^T) X_1) + N X_2 (\gamma^{-2} B_1 B_1^T - B_2 B_2^T) X_2 + P^T P = 0. \quad (4.7)$$

Taking into consideration the state-feedback gain matrix structure, namely,

$$\tilde{F} = \begin{bmatrix} F_1 & F_2 & \cdots & F_2 \\ F_2 & F_1 & \cdots & F_2 \\ \vdots & \vdots & \ddots & \vdots \\ F_2 & F_2 & \cdots & F_1 \end{bmatrix} \quad (4.8)$$

the optimal state-feedback gains have the following expressions:

$$\begin{aligned} F_1 &= -B_2^T (X_1 + (N-1)X_2) \\ F_2 &= B_2^T X_2. \end{aligned} \quad (4.9)$$

4.3 Distributed Control

In the centralised controller case, where all agents are interconnected, the adjacency matrix has all extra-main diagonal elements equal to 1. Due to the limited information transmission between network members, in the case of distributed controller, its expression can be written using the adjacency matrix as:

$$\tilde{F}_D = I_N \otimes F_1 + \mathcal{A}(\mathcal{G}) \otimes F_2. \quad (4.10)$$

The existence of null terms in the adjacency matrix introduces a new problem, namely, if the obtained distributed controller guarantees the system stability and ensures the required H_∞ performances. Adopting the parameterization in [6]

$$\tilde{F}_D = I_N \otimes F_1 + a I_N \otimes F_2 + b \mathcal{A}(\mathcal{G}) \otimes F_2 \quad (4.11)$$

the parameters a and b range is determined so that the closed-loop multi-agent system stability is obtained. Considering the notation $\mu_i, i = 1, \dots, N$ corresponding to the adjacency matrix $\mathcal{A}(\mathcal{G})$ eigenvalues, the following algorithm proposed in [11] is used to determine the necessary parameters to maintain the stability properties.

Step 1. Determine $\delta_1 < 0$ and $\delta_2 > 0$ such that $\Lambda(\tilde{A}_D) \in \mathbb{C}^-, \forall \delta \in [\delta_1, \delta_2]$;

Step 2. Solve the systems of inequalities

$$\begin{aligned} \delta_1 + 1 - N_L + a + b\bar{\mu} &< 0 \\ \delta_2 + 1 - N_L + a + b\underline{\mu} &> 0 \\ b &> 0 \end{aligned} \quad (4.12)$$

and

$$\begin{aligned} \delta_1 + 1 - N_L + a + b\bar{\mu} &< 0 \\ \delta_2 + 1 - N_L + a + b\underline{\mu} &> 0 \\ b &< 0 \end{aligned} \quad (4.13)$$

where $\underline{\mu} = \min_i \mu_i$ and $\bar{\mu} = \max_i \mu_i$.

5 Case Studies - H_∞ Design

The second design method analysed in this work, named H_∞ , assumes specific properties, requiring the definition of system equations for the considered network of form (4.1).

5.1 H_∞ Design in case of ideal communication channels

5.1.1. Centralised Control

- Longitudinal Dynamics

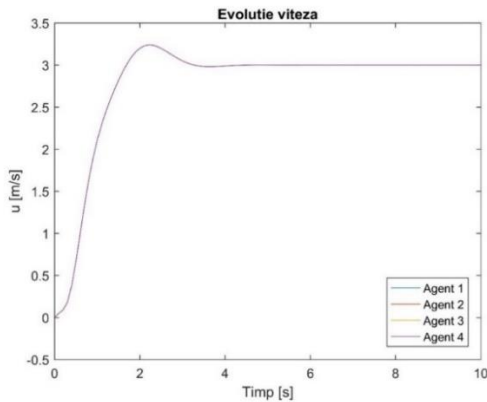


Figure 5.1 Time evolution of velocity – centralised control

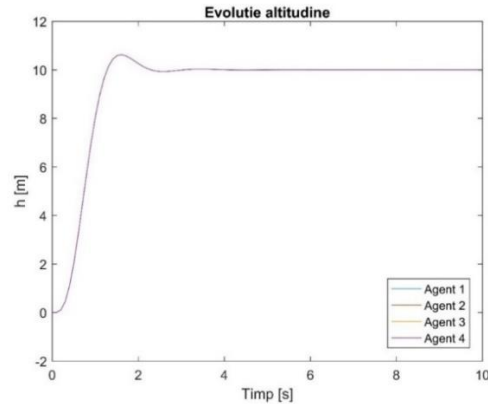


Figure 5.2 Time evolution of altitude – centralised control

Figure 5.1 represents the time evolution of velocity for the entire network for which it is required to reach and maintain the pre-set value $u = 3 \text{ m/s}$. Figure 5.2 illustrates the time evolution of altitude for the four agents of the interconnected system.

- **Lateral Dynamics**

In the case of lateral dynamics, the time responses of velocity and altitude are analysed. Figure 5.3 shows the time response of velocity where the networked members are observed to reach the imposed value, maintaining it throughout the simulation, taking into consideration the different initial conditions. Figure 5.4 demonstrates the network capacity to stabilise at the desired yaw angle value.

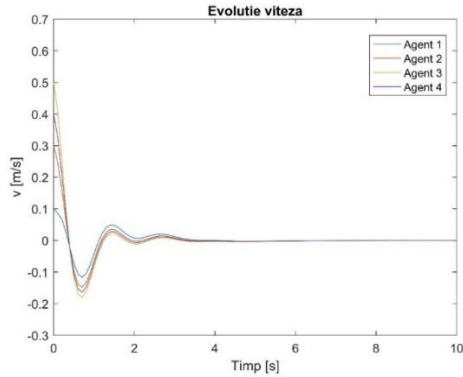


Figure 5.3 Time evolution of velocity – centralised control

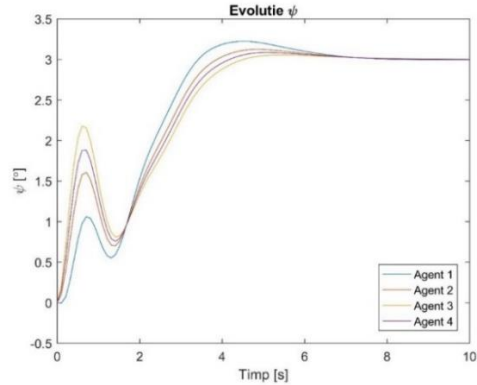


Figure 5.4 Time evolution of ψ – centralised control

5.1.2. Distributed Control

- ❖ **Longitudinal Dynamics**

- **Configuration B**

This part analyses the behaviour of the configuration in Figure 3.6, where all agents have an equal number of connections. Figure 5.5 shows the time evolution of velocity for which the imposed value $u = 3 \text{ m/s}$ is reached. Although the information transmission between certain pairs of agents is limited, the obtained distributed controller guarantees the system stability.

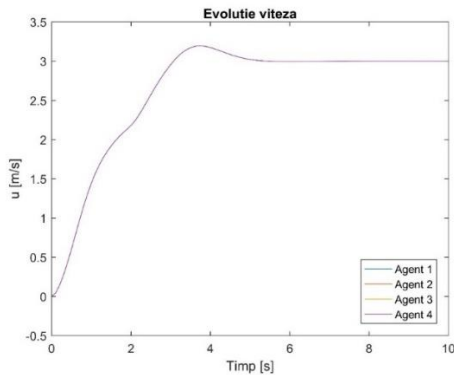


Figure 5.5 Time evolution of velocity – distributed control – Config. B

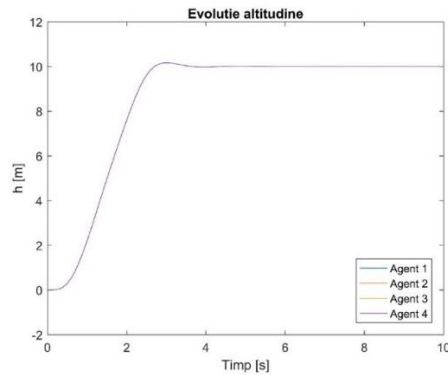


Figure 5.6 Time evolution of altitude – distributed control – Config. B

- **Configuration F**

It is important to study the case where the maximum number of an agent connections considerably increases. Thus, the configuration in Figure 5.7 is considered, where $d_{max} = 7$ for agent 1 and agent 2. Maintaining the same imposed conditions in the other analysed cases, the time responses of velocity and altitude shown in Figure 5.8 and Figure 5.9 are obtained.

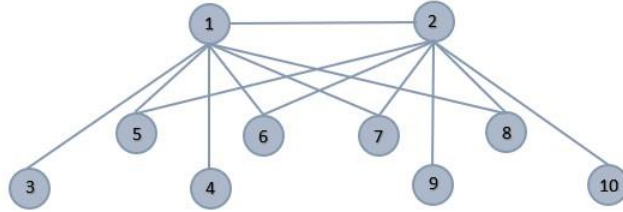


Figure 5.7 Configuration F

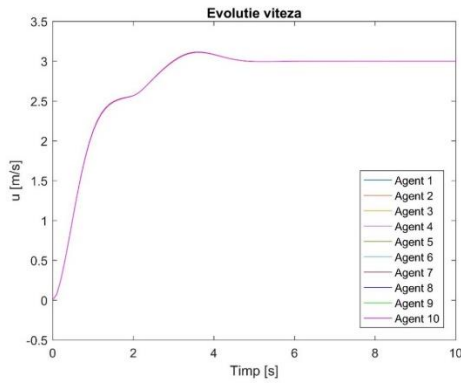


Figure 5.8 Time evolution of velocity – distributed control – Config. F

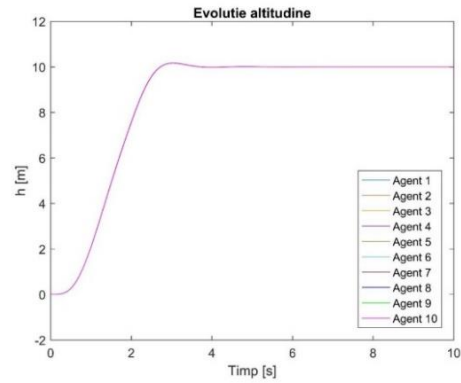


Figure 5.9 Time evolution of altitude – distributed control – Config. F

- ❖ **Lateral Dynamics**

- **Configuration F**

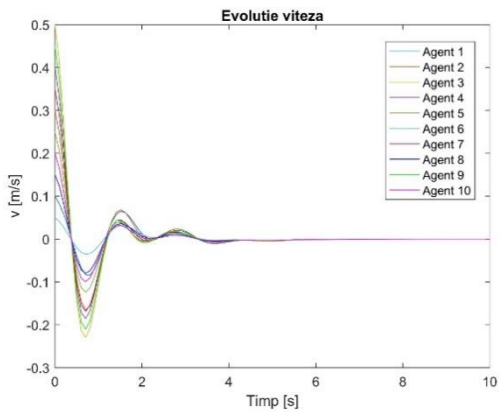


Figure 5.10 Time evolution of velocity – distributed control – Config. F

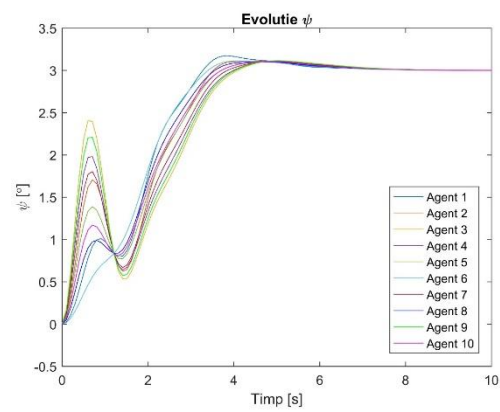


Figure 5.11 Time evolution of ψ – distributed control – Config. F

To obtain the numerical simulations, the initial conditions considered in the previous cases are maintained. The time evolution of velocity shown in Figure 5.10 highlights the different initial values of the network agents and the null value maintenance throughout the simulation. The time evolution of yaw angle (Figure 5.11) reflects the controller capacity to obtain network stability, achieving the desired objectives.

5.2 H_∞ Design in case of time delays communication network

Although time delays are a recent topic in recent literature, the challenge consists of developing control algorithms for aerial vehicles networks considering their effects. Thus, their impact on the decoupled dynamics of the vehicles is analysed, for different considered configurations. Hence, to analyse their influences, the first-order delay modelled with the Padé approximation is considered.

5.2.1. Centralised Control

The time evolutions of the states corresponding to the decoupled dynamics of the vehicles reflect distinct behaviours for the two situations (the time-delays case and the ideal one). The presence of the considered time delay is reproduced by the offset between the two graphical representations, without affecting the network stability.

5.2.2. Distributed Control

❖ Longitudinal Dynamics

• Configuration F

Maintaining the same conditions imposed in the other analysed cases, the comparative graphic representations of the two states are obtained, illustrated in Figure 5.12 and Figure 5.13. The offset caused by the time-delays is observed, without affecting the network stability and the desired objectives achievement.

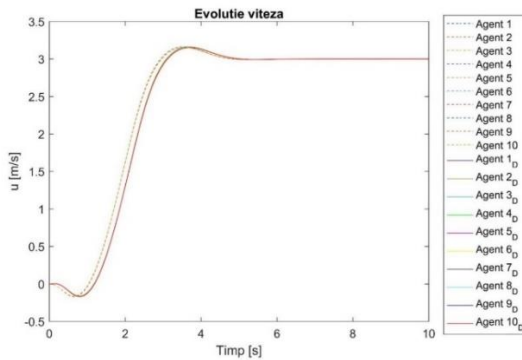


Figure 5.12 The comparative time evolutions of velocity – distributed control – Config. F

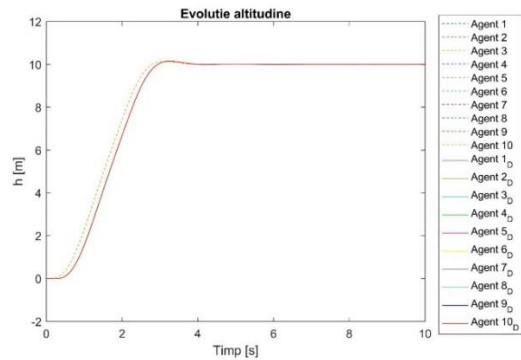


Figure 5.13 The comparative time evolutions of altitude – distributed control – Config. F

❖ Lateral Dynamics

• Configuration F

In this part, it is desired to study the time-delays influences in a flight configuration case where the maximum number of connections of an agent significantly increases. Like the previous situations, the comparative time evolutions of velocity (Figure 5.14) and yaw angle (Figure 5.15) for each member are presented, where the offset due to the time delay is noted. The maximum reached value of the yaw angle corresponds to the agent 3 for which the initial velocity condition is maximum. Their progressive decrease is achieved according to the different initial velocity values.

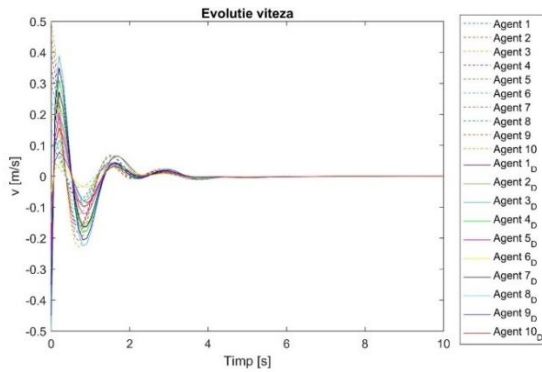


Figure 5.14 The comparative time evolutions of velocity – distributed control – Config. F

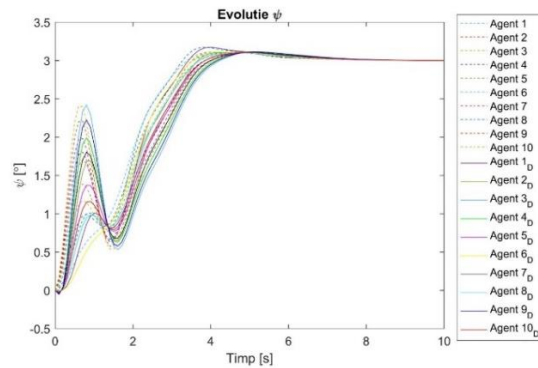


Figure 5.15 The comparative time evolutions of ψ – distributed control – Config. F

5.3 H_∞ Design in case of failure communication

Communication between agents plays an essential role in the automatic control system design. The data transmission can have an impact on the entire flight formation, therefore different situations involving interconnection failure are analysed. To study the time evolutions of the networked agents, the decoupled dynamics of two flight formations whose configurations are illustrated in Figure 5.16 (configuration C) and Figure 5.7 (configuration F) are considered. The interconnected systems equations, the initial conditions and the imposed objectives are the same as detailed for the ideal communication case.

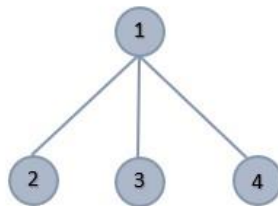


Figure 5.16 Configuration C

5.3.1. Situation I

The first analysed situation consists in the certain agents failure case. For the configuration in Figure 5.16, the failure of agent 2 is considered and for the Figure 5.7, the connection with agent 2 and agent 5 is not possible.

- **Longitudinal Dynamics**

Firstly, the time evolutions of the two analysed states of configuration C are obtained, which are represented in Figure 5.17 and Figure 5.18. The simulations illustrate the detailed behaviour of the entire network in order to highlight the influence of agent 2 failure on the other agents. It can be seen that the connection loss of agent 2 has no significant effects on the network stability or the imposed objective achievement. This fact is highlighted by the small differences in the state evolutions in the mentioned period.

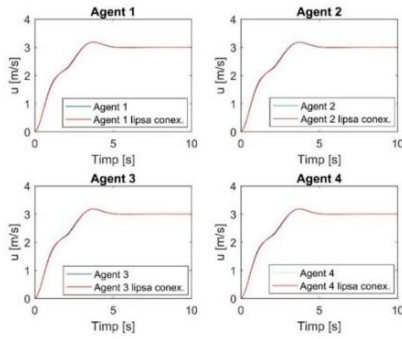


Figure 5.17 Time evolution of velocity for config. C – agent 2 failure

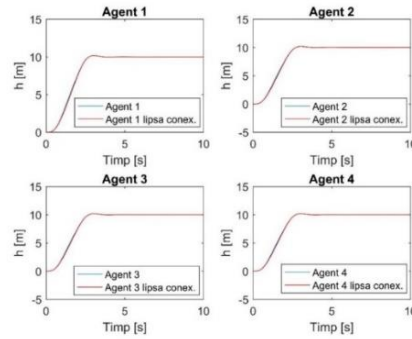


Figure 5.18 Time evolution of altitude for config. C – agent 2 failure

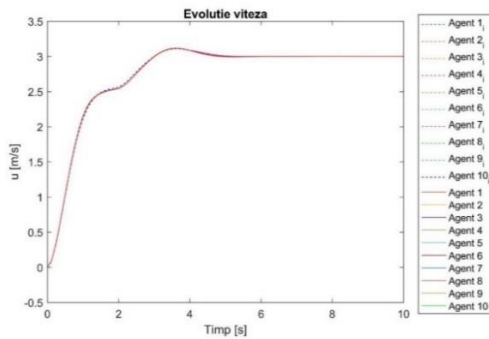


Figure 5.19 Time evolution for velocity for config. F – agent 2 and agent 5 failure

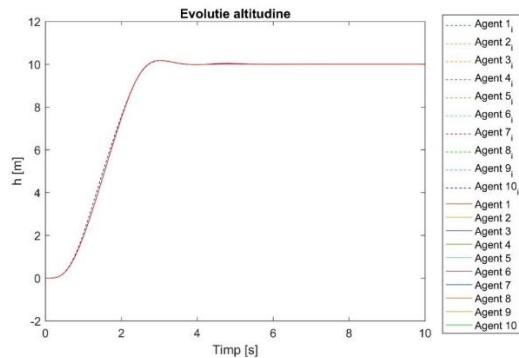


Figure 5.20 Time evolution of altitude for config. F – agent 2 and agent 5 failure

Analysing the time evolutions of the two states of configuration F (Figure 5.19 and Figure 5.20), differences in member behaviours are identified not only for the considered period. Considering the maximum number of connections for agent 2, the effects are not significant. Therefore, network stability and desired performance are obtained.

- **Lateral Dynamics**

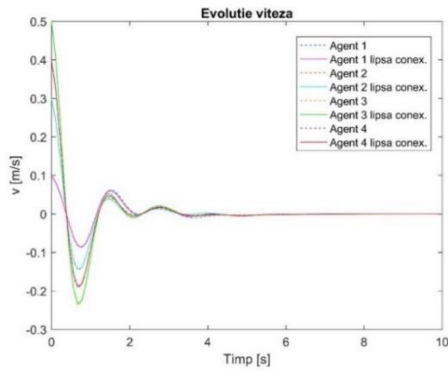


Figure 5.21 Time evolution of velocity for config. C – agent 2 failure

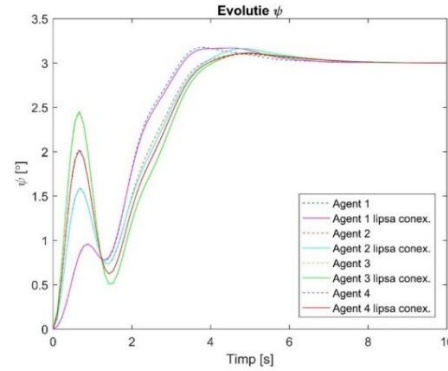


Figure 5.22 Time evolution of yaw angle for config. C – agent 2 failure

From the graphical representations of the analysed states corresponding to the lateral dynamics presented in Figure 5.21 and Figure 5.22, it can be observed that the communication loss with agent 2, for a pre-set period, does not affect the desired performances. In the case of the configuration with a larger number of agents (configuration F), the comparative representations for both situations (ideal communication and imperfect connections) are illustrated in Figure 5.23 and Figure 5.24.

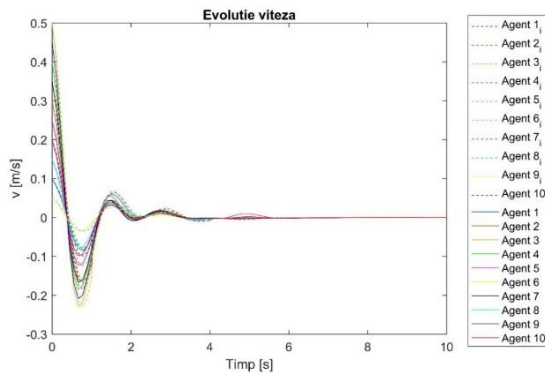


Figure 5.23 Time evolution of velocity for config. F – agent 2 and agent 5 failure

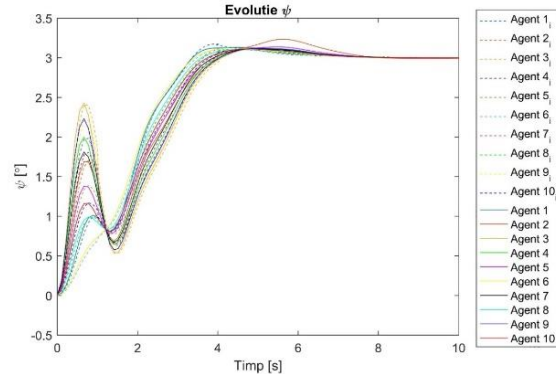


Figure 5.24 Time evolution of yaw angle for config. F – agent 2 and agent 5 failure

5.3.2. Situation II

In the second studied scenario, the complete communication loss for the same limited period is considered. This case is analysed for the two above-mentioned configurations.

- **Longitudinal Dynamics**

The time evolutions of velocity (Figure 5.25) and altitude (Figure 5.26) are obtained, where the index i denotes the states of the ideal case. It is noted that the effects of complete

communication loss for a determined period continue for a while after connections are re-established. These aspects do not have a negative impact on desired performance.

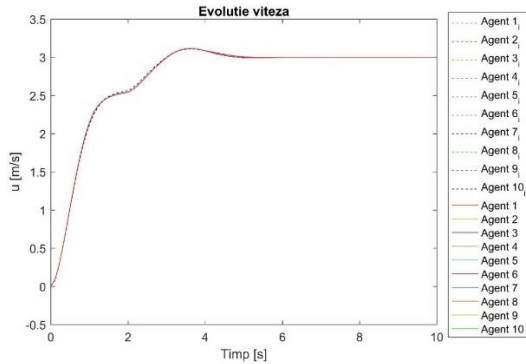


Figure 5.25 Time evolution of velocity for config. F – complete communication failure

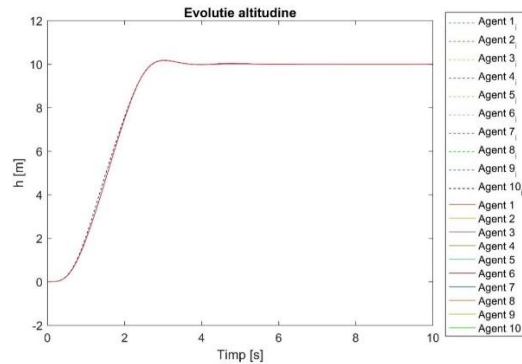


Figure 5.26 Time evolution of altitude for config. F – complete communication failure

- **Lateral Dynamics**

Similar to the previous situation, identical objectives are considered for the two different flight configurations, maintain the same periods of complete connections loss. The time evolutions of the states for the first configuration are presented in Figure 5.27 and Figure 5.28.

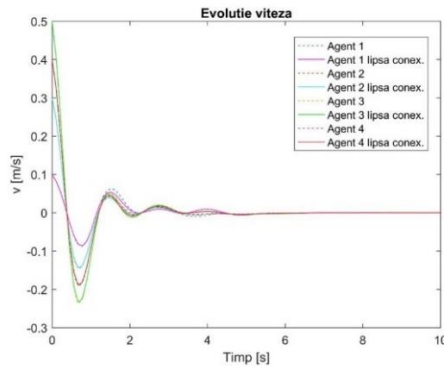


Figure 5.27 Time evolution of velocity for config. C - complete communication failure

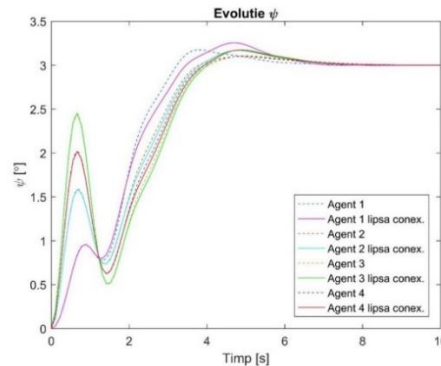


Figure 5.28 Time evolution of yaw angle for config. C - complete communication failure

6 H_∞ Design for stochastic systems with Markov Chains

In this part, the H_∞ controller design for multi-agent systems with identical dynamics is considered, where the data loss in communication networks is represented by the Markov process. These models are used for the simulation and modelling of communication systems, addressed in works such as [12], [13], [14].

6.1 Case of single agent

The following linear stochastic system is considered

$$\begin{aligned}\dot{x}(t) &= A(\eta(t))x(t) + B_1(\eta(t))u_1(t) + B_2(\eta(t))u_2(t) \\ y_1(t) &= C(\eta(t))x(t) + D(\eta(t))u_2(t) \\ y_2(t) &= x(t)\end{aligned}\tag{6.1}$$

where the notations for system (4.1) hold and $\eta(t), t \geq 0$ denotes the continuous Markov chain with the state space $\mathcal{D} = \{1, \dots, d\}$ and $P(t) = [p_{ij}(t)] = e^{It}, i, j \in \mathcal{D}, t \geq 0$ is the probability transition matrix in which the stationary transition rate matrix of η is $\Pi = [\pi_{ij}]$ with $\sum_{j=1}^d \pi_{ij} = 0, i \in \mathcal{D}$ and $\pi_{ij} \geq 0$ if $i \neq j$.

Definition 1 [15]. The stochastic system with Markov parameters

$$\dot{x}(t) = A(\eta(t))x(t)\tag{6.2}$$

is exponentially stable in mean square (ESMS) if there exists $\beta \geq 1$ and $\alpha > 0$ such that $E[|\Phi(t)|^2 | n(0) = i] \leq \beta e^{-\alpha t}, \forall t \geq 0, i \in \mathcal{D}$, where $\Phi(t)$ represents the fundamental (random) solution of the differential system (6.2).

Theorem 3 [15]. If the system of coupled Riccati equations

$$\begin{aligned}A^T(i)X(i) + X(i)A(i) + X(i)(\gamma^{-2}B_1(i)B_1^T(i) - B_2(i)B_2^T(i))X(i) + \sum_{j=1}^d \pi_{ij}X(j) + \\ C^T(i)C(i) = 0\end{aligned}\tag{6.3}$$

has a stabilising solution $(X(1), \dots, X(d))$ with $X(i) \geq 0, \forall i \in \mathcal{D}$ for a certain value $\gamma > 0$, and namely, if the stochastic system with Markov chains

$$\dot{x}(t) = \left(A(\eta(t)) + \left(\gamma^{-2}B_1(\eta(t))B_1^T(\eta(t)) - B_2(\eta(t))B_2^T(\eta(t)) \right) X(\eta(t)) \right) x(t)$$

is ESMS, where

$$F(\eta(t)) = -B_2^T(\eta(t))X(\eta(t)),\tag{6.4}$$

then the control law $u(t) = F(\eta(t))x(t)$ stabilises the system (6.1) and

$$E\left[\int_0^\infty (|y_1(t)|^2 - \gamma^2|u_1(t)|^2) dt\right] \leq 0\tag{6.5}$$

for $\forall u_1 \in L_\eta^2([0, \infty), \mathcal{R}^{m_1})$, where the quality output $y_1(t)$ is determined with the initial condition $x(0) = 0$ of the system (6.1).

6.2 Multi-agent systems

Theorem 4. (i) If the system of coupled Riccati equations

$$\begin{aligned}\tilde{A}^T(i)\tilde{X}(i) + \tilde{X}(i)\tilde{A}(i) + \tilde{X}(i)\left(\gamma^{-2}\tilde{B}_1(i)\tilde{B}_1^T(i) - \tilde{B}_2(i)\tilde{B}_2^T(i)\right)\tilde{X}(i) + \\ \sum_{j=1}^d \pi_{ij}\tilde{X}(j) + \tilde{Q}^T(i)\tilde{Q}(i) = 0, i = 1, \dots, d\end{aligned}\tag{6.6}$$

has a positive semidefinite stabilising solution $(\tilde{X}(1), \dots, \tilde{X}(d))$ with $\tilde{X}(i) \geq 0, i = 1, \dots, d$, then the stochastic system with Markov parameters

$$\dot{\hat{x}}(t) = \left(\tilde{A}(\eta(t)) + \tilde{B}_2(\eta(t))\tilde{F}(\eta(t)) \right) x(t) + \tilde{B}_1(\eta(t))\tilde{u}_1(t) \quad (6.7)$$

where $\tilde{F}(i) = -\tilde{B}_2^T(i)\tilde{X}(i)$, $i = 1, \dots, d$, is ESMS and for the initial condition $\hat{x}(0) = 0$,

$$E\left[\int_0^\infty (|\tilde{y}_1(t)|^2 - \gamma^2|\tilde{u}_1(t)|^2) dt\right] \leq 0$$

for all $\tilde{u}_1 \in L_\gamma^2([0, \infty), \mathcal{R}^{N \cdot m_1})$.

(ii) The solution of equation (6.6) has the following structure:

$$\begin{aligned} \tilde{X}(i) &= [\tilde{X}_{k\ell}]_{k,\ell=1,\dots,N} \text{ where} \\ \tilde{X}_{kk}(i) &= X_1(i) + (N-1)X_2(i) \\ \tilde{X}_{k\ell}(i) &= -X_2(i), k, \ell = 1, \dots, N, k \neq \ell \end{aligned} \quad (6.8)$$

and $(X_1(1), \dots, X_1(d))$, $(X_2(1), \dots, X_2(d))$ are the solutions of Riccati equations

$$\begin{aligned} A^T(i)X_1(i) + X_1(i)A(i) + X_1(i)(\gamma^{-2}B_1(i)B_1^T(i) - B_2(i)B_2^T(i))X_1(i) + \\ \sum_{j=1}^d \pi_{ij}X_1(j) + C^T(i)C(i) = 0, i = 1, \dots, d \end{aligned} \quad (6.9)$$

and

$$\begin{aligned} [A(i) + (\gamma^{-2}B_1(i)B_1^T(i) - B_2(i)B_2^T(i))X_1(i)]^T X_2(i) + X_2(i)[A(i) + \\ (\gamma^{-2}B_1(i)B_1^T(i) - B_2(i)B_2^T(i))X_1(i)] + NX_2(i)(\gamma^{-2}B_1(i)B_1^T(i) - \\ B_2(i)B_2^T(i))X_2(i) + \sum_{j=1}^d \pi_{ij}X_2(j) + P^T(i)P(i) = 0, i = 1, \dots, d. \end{aligned} \quad (6.10)$$

(iii) If the Riccati systems (6.9) and (6.10) have the stabilising solutions $(X_1(1), \dots, X_1(d))$ and $(X_2(1), \dots, X_2(d))$, with $X_1(i) \geq 0$ and $X_2(i) \geq 0$, $i = 1, \dots, d$ then $(\tilde{X}(1), \dots, \tilde{X}(d))$ with $\tilde{X}(i)$ defined in (6.8) is the stabilising solution of system (6.6) and $\tilde{X}(i) \geq 0$, $i = 1, \dots, d$.

7 Case Studies - H_∞ Design with Markov Chains

In this part, two cases of the Markov process ($\mathcal{D} = \{1,2\}$) are considered and namely, $i = 1$, the nominal case, where all networked agents are interconnected, and $i = 2$, the case corresponding to the loss of connections. The matrix Π is chosen with the following numerical values:

$$\Pi_1 = \begin{bmatrix} -0.5 & 0.5 \\ 0 & 0 \end{bmatrix}. \quad (7.1)$$

Figure 7.1 illustrates the transition probabilities from the nominal case to the connection loss one, corresponding to the transition matrix Π_1 .

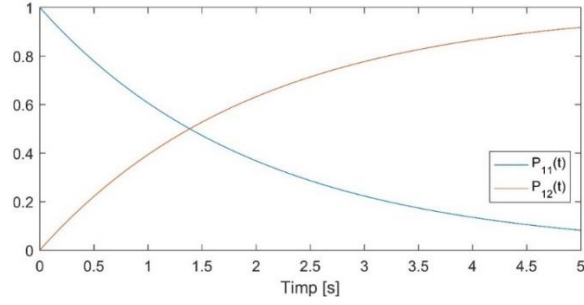


Figure 7.1 Transition probabilities Π_1

7.1 $N = 100$ agents

Aiming to illustrate the theoretical notions for an extended configuration, as in [15], a network with 100 identical agents is chosen, for which the kinematic equations with the following expressions are considered:

$$\begin{aligned} \ddot{x}_k(t) &= u_k(t) \\ \ddot{y}_k(t) &= v_k(t), \quad k = 1, \dots, N \end{aligned} \quad (7.2)$$

where x_k and y_k represent the Cartesian coordinates and u_i and v_i denote their commanded accelerations. Considering that the quality outputs vector has the form $y_{1k} = [x_k \ y_k \ u_k \ v_k]^T$, the corresponding matrices to the equations system (6.1) are identical for both cases of the Markov process. Solving the Riccati systems (6.9) and (6.10) for $\gamma = 100$, the necessary gains to obtain the agents trajectories for both considered situations are acquired.

Figure 7.2 presents snapshots at different time ($t = 0.5$ s and $t = 2$ s) of agents evolutions, for which random initial positions are considered and the main objective is their arrangement in a certain frame, similar to the square geometric shape. The two figures in the upper half demonstrate the importance of the P matrix denoting the coupling mode of the agents for achieving the predetermined objective in a reduced time. Numerical simulations show that communication failure causes an increase of the required time to approximately 6.5 s.

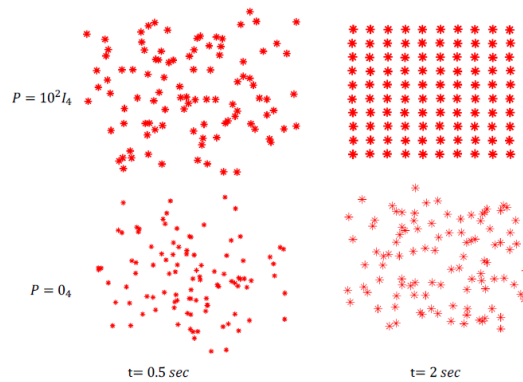


Figure 7.2 Snapshots of agents position simulations

7.2 $N = 3$ agents

A flight configuration consisting of 3 identical agents, shown in Figure 7.3, is considered, for which both dynamics are analysed.

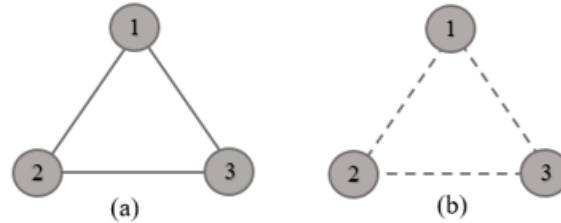


Figure 7.3 Network configuration with Markov chains

- **Longitudinal Dynamics**

In Figure 7.4, an offset between the case where all members are interconnected ($i = 1$) and the situation where all connections are lost ($i = 2$) is noticed. The time evolutions of the three agents are similar in both scenarios. Taking into account the initial imposed values, the imposed performances achievement is observed for both the situation where the communication is possible and the case of complete loss of connections. For the time evolution of altitude (Figure 7.5), it is noticed that the desired values have been reached for the interconnected members. Therefore, different behaviours are marked for the cases $i = 1$ and $i = 2$.

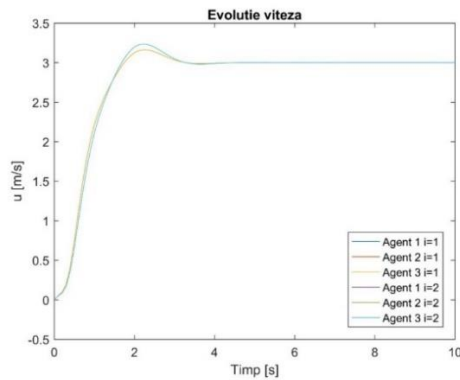


Figure 7.4 The time evolution of agents velocity for both cases

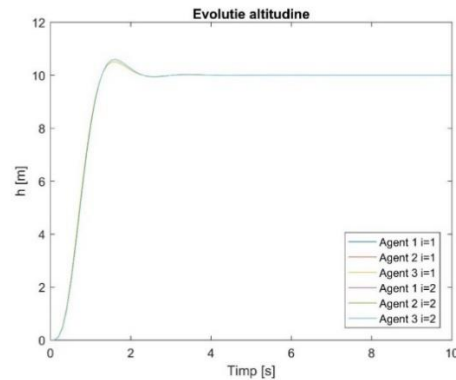


Figure 7.5 The time evolution of agents altitude for both cases

- **Lateral Dynamics**

For the situation in which all agents are interconnected, the time evolution of velocity in Figure 7.6 is obtained. Different behaviours are identified depending on the different initial values. This observation is also found in the case of interconnection loss (Figure 7.7), but the velocity variations in this situation are wider. Analysing the time behaviour in terms of yaw angle (Figure 7.8 and Figure 7.9), it can be noticed that the evolution variations are more pronounced for the $i = 2$ case.

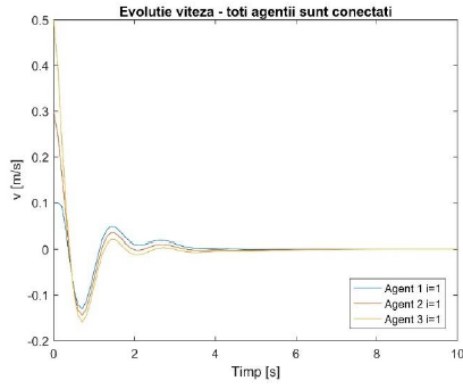


Figure 7.6 Time evolution of velocity for nominal case ($i=1$)

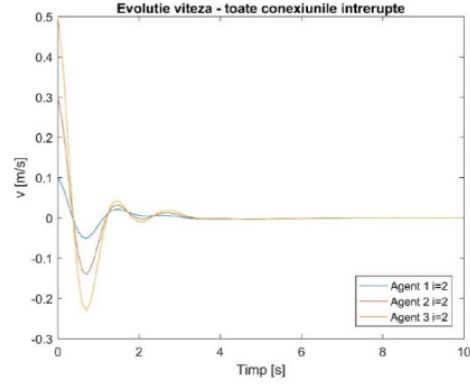


Figure 7.7 Time evolution of velocity for communication loss case ($i=2$)

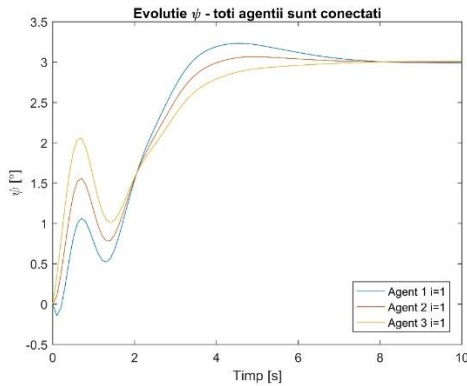


Figure 7.8 Time evolution of yaw angle for nominal case ($i=1$)

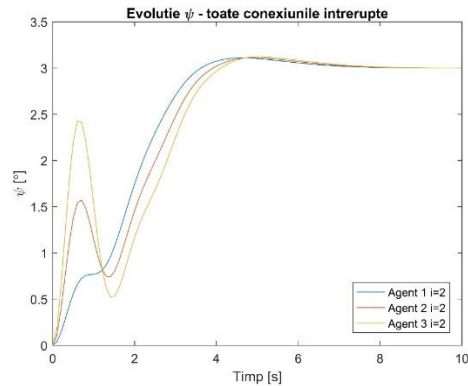


Figure 7.9 Time evolution of yaw angle for communication loss case ($i=2$)

8 Results and Concluding Remarks

In the present work, the attention is focused on the problem of multi-agent control systems, thus distinct approaches of optimal control are considered. One of the specific challenges faced by this type of systems concerns the information transmission between agents, which is possible due to the communication channels. On the other hand, this feature implies different imperfections of the transmission channels that can have some effects as: reducing the desired performances or influencing the network stability. Knowing the importance of studying these factors influence (the failure of certain agents, the presence of time-delays, the transmission channels overloading that cause data packet drop off) on the interconnected system stability, it is relevant to analyse the agents' responses in these situations.

The time-delays introduction is represented by the offset between the case with communication channels imperfections and the ideal one. Looking at the necessary time to stabilise at the imposed values, the sensitivity of the last configuration to delays is observed, where slower evolutions are identified. In the case of certain members failure, obvious changes are

identified in the case of agents with maximum connections number and whose communication becomes impossible to achieve.

First, in order to highlight the capabilities of H_∞ design with Markov processes, an extended configuration with 100 agents with identical dynamic is considered, using the kinematic equations. The designed controller capacity to stabilise a network with a significant number of agents ($N = 100$) and to ensure the desired performances are presented for the kinematic equations system. With random values of the initial positions of the members, the network response is shown for both the nominal case and the case where the communication is not available. It is observed that the complete loss of connections causes an increase in the required time for stabilisation.

Regarding the configuration with reduced number of agents, the offset between the nominal case ($i = 1$) and the situation where all links fail ($i = 2$) is remarked. The agents stabilisation at the desired value, maintained throughout the simulation, is slower for the case where the communication between members is lost. The most pronounced variations of both states are observed in the case when communication fails ($i = 2$).

9 References

- [1] *P. Massioni, M. Verhaegen* – “Distributed Control for Identical Dynamically Coupled Systems: A Decomposition Approach”, IEEE Transactions on Automatic Control, 2009.
- [2] *Y. Cao, W. Yu, W. Ren, G. Chen* – “An Overview of Recent Progress in the Study of Distributed Multi-Agent Coordination”, IEEE Transactions on Industrial Informatics, 2013.
- [3] *S. Knorn, Z. Chen, R. Middleton* – “Overview: collective control of multi-agent systems”, IEEE Transactions Control Networked Systems, 2016.
- [4] *B. D. O. Anderson, J. B. Moore* – “Optimal Control. Linear Quadratic Methods”, 1989.
- [5] *C. Godsil, G. Royle* – „Algebraic Graph Theory”, Springer Science & Business Media, 2001.
- [6] *F. Borelli, T. Kevinczky* – “Distributed LQR design for identical dynamically decoupled systems”, Proceedings of the 45th IEEE Conference on Decision & Control, USA, 2006.
- [7] *C. Hajiyeve, H. E. Soken, S. Y. Vural* – „State Estimation and Control for Low-cost Unmanned Aerial Vehicles”.
- [8] *K. Zhou, J. C. Doyle, K. Glover* – „Robust and Optimal Control”, Prentice Hall, 1996.
- [9] *C. Scherer* – „Theory of Robust Control”, 2001.
- [10] *A. Stoorvogel* – „The H_∞ Control Problem: A State Space Approach”, 2000.
- [11] *A. – M. Stoica* – „ H_∞ Type Control for Multi-Agent Systems subject to Stochastic State Dependent Noise”, SICON.
- [12] *A. Konrad, B. Y. Zhao, A. D. Joseph, R. Ludwig* - „A Markov-based channel model algorithm for wireless networks”, 2003.

- [13] *Y. Zhou, L. Lamont, C. A. Rabbath* – „A Markov-Based Packet Dropout Model for UAV Wireless Communications”, 2012.
- [14] *S. Primak, V. Kontorovitch, V. Lyandres* – „Stochastic Methods and their Applications to Communications”, 2014.
- [15] *A.-M. Stoica, S. C. Stoicu* – „ H_∞ State-Feedback Control of Multi-Agent Systems with Data Packet Dropout in the Communication Channels: A Markovian Approach”, MDPI Journal, 2022.